Development of paper-based biosensors for DNA recognition and proteolytic activity

Hélvio Miguel Rodrigues Simões[1]
[1]IBB – Institute for Bioengineering and Biosciences, Instituto Superior Técnico, Universidade de Lisboa, Lisbon, Portugal

Abstract

The design of new diagnostic solutions that are more affordable and easier to manage is of great interest for economic and health safety reasons. These tests should be simple, portable and require small sample volumes with little to no preparation, so they can be used at the point of care (POC) without the need for elaborate equipment. The ubiquity and ease of handling of paper make it an excellent support for such tests. One strategy to achieve this goal is to combine paper with gold nanoparticles (AuNPs), which produce a colorimetric signal visible to the naked eye. In this work, two tests were developed using AuNPs detection by bioactivating cellulose with the carbohydrate binding module CBM3-C. This protein was thoroughly characterized and employed for sensing: a) complementary DNA (cDNA) capture and b) proteolytic activity. For cDNA recognition, a capture oligonucleotide was conjugated with CBM3-C using two different strategies: i) the formation of a nickel complex with trisNTA-modified oligonucleotides via the hexa-histidine tag of CBM3-C and ii) the formation of a covalent bond between the terminal thiol moiety of CBM3-C and maleimide-modified oligonucleotides. Recognition of cDNA by the conjugates was performed in a wax-printed microfluidic device both directly and indirectly, using a 2- or 3-oligonucleotide system, respectively. The nickel complex conjugate was able to accurately detect cDNA in the 2-oligonucleotide system, but the covalent conjugate was less discriminatory. Both conjugates returned positive signals in assays without the target strand. CBM3-C was also successfully used in a proof-of-concept assay for measurement of the extent of a proteolytic reaction using a non-specific protease.

Keywords: Biosensor, Paper-Based Devices, Gold Nanoparticles, Carbohydrate-Binding Module, DNA recognition, Proteolytic Activity

1. Introduction

In an ever-changing world, the search for faster, more reliable and affordable methods of diagnosis is paramount. Better diagnostics would be of major support in several areas, e.g. environmental safety, food and water quality testing and disease control. As these three areas are highly interconnected, a rampant uncontrolled outbreak can lead to serious problems worldwide. In the 21st century, the Commission on a Global Health Risk Framework for the Future expect that over $6 trillion will be necessary for pandemic disease event response[1]. To curtail such costs, diagnostic methods should follow the World Health Organization's ASSURED criteria: Affordable, Sensitive, Specific, User-friendly, Rapid and robust, Equipment-free and Deliverable to end-users[2]. Point-of-care (POC) tests meet these conditions, besides requiring small amounts of sample with low analyte concentration and little to no preparation.

In an attempt to cut production costs, facilitate scalability and improve usability, POC diagnostics have been developed using paper[3], which displays a set of very convenient features: (i) it has an inherent ability to wick fluids, i.e., it is able to transport fluids without the need for external pumping; (ii) it can hold/store active reagents in its fiber network; (iii) its high surface area to volume ratio improves detection limits, e.g. if a colorimetric method is used; (iv) it can be easily modified, whether by cutting and folding or by chemical treatment; (v) it is easy to scale by printing; and (vi) it is easy to dispose of by incineration. Microfluidic paper-based analytical devices (µPADs) can be created by defining boundaries in a paper strip by printing with a wax-based ink, for example, creating an arrangement of channels and target areas that guide and confine fluids in the device. Then, a bioreceptor is immobilized in a designated spot in order to accurately capture the analyte. Subsequent events involving secondary reagents ultimately produce an observable and measurable signal, thus confirming detection. Among other methods, conjugation of bioreceptors with a carbohydrate-binding module (CBM) with cellulose affinity (e.g. CBM3 from *Clostridium thermocellum*) allows accurate immobilization and avoids non-specific binding.

CBMs are contiguous sequences of amino acid residues with structurally discrete folds and carbohydrate-binding activity[4–6]. They do not possess any catalytic activity themselves, but are often found accompanying catalytic domains, directing them to their substrate[7]. CBMs are available in several different folds, with the most common being the β-sandwich. Several biosensors based on CBMs have been developed, namely for the recognition of *E. coli* cells[8,9] and in immunoassays for DNA recognition[10,11].

For detection purposes, several methods can be employed. Colorimetric sensing, in which the analyte presence in confirmed by the production of color, is one of the simplest and best suited for POC applications. One colorimetric method is based on gold nanoparticles (AuNPs)[12], whose size, shape and surrounding chemical environment can be adjusted to the desired outcome. Besides, they display excellent biocompatibility, good stability, ease of functionalization with biomolecules, appropriate optoelectronic properties, and a distinctive red hue. The latter is key to providing a first-hand qualitative analysis or even a possible quantitative analysis.

The main objective of this work is to develop tests for POC applications based on colorimetric detection with AuNPs and a new CBM3-based construct: CBM3-C, which contains an N-terminal hexa-histidine tag and a C-terminal cysteine (Figure 1). The first application is for recognition of DNA, in which a CBM3-C:DNA conjugate is the biorecognition element and the complementary target DNA strand is immobilized on AuNPs (Figure 2).

CBM3-C – *184 aa, 20.2 kDa*

MGSSHHHHHHSSGPQQGLRANTPVSGNLKVE
FYNSNPSDTTNSINPQFKVTNTGSSAIDLSK
LTLRYYYTVDGQKDQTFWCDHAAIIGSNGSY
NGITSNVKGTFVKMSSSTNNADTYLEISFTG
GTLEPGAHVQIQGRFAKNDWSNYTQSNDYSF
KSASQFVEWDQVTAYLNGVLVWGKEPGGC

Figure 1: Amino acid sequence of the recombinant protein CBM3-C. Blue – hexa-histidine tag; Green – CBM3 from *Clostridium thermocellum*; Red – linker. The residues involved in the binding of CBM3 to cellulose are underlined and the cysteine residues are doubly underlined.

The second application is focused on the detection of proteolytic activity. Pre-incubation of CBM3-C with non-specific proteases (e.g., trypsin) breaks the connection between cellulose nanoparticles and AuNP that bind to thiol groups established by the CBM3-C, due to proteolysis. The measurement of AuNPs in the supernatant of a cellulose nanoparticle suspension after particle deposition allows for analysis of proteolytic cleavage extent (Figure 3).

2. Materials and Methods

2.1. Device fabrication

µPADs were developed on Whatman no.1 chromatography paper. The boundaries were defined by wax printing with a Xerox ColorQube 8570 color printer, according to the established

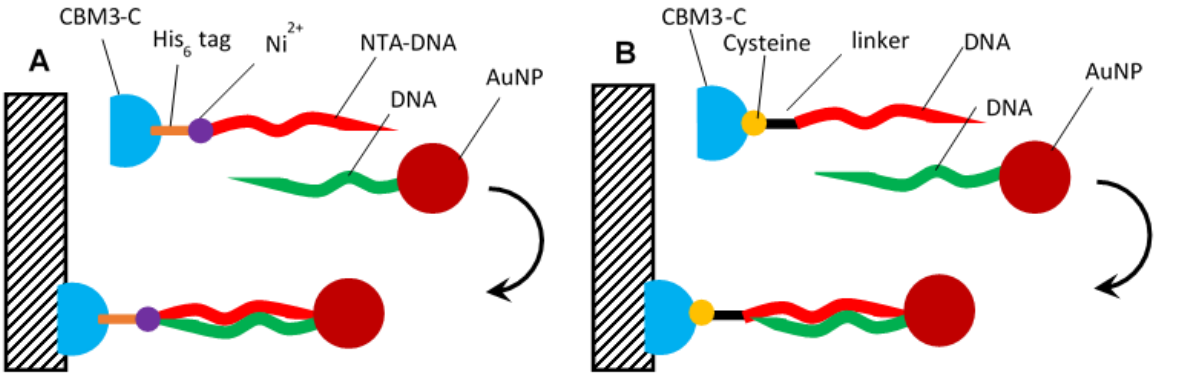

Figure 2: Schematic representation of the two approaches used to develop DNA paper-based DNA detection system. A: Non-covalent binding of DNA to CBM3-C. An NTA-modified DNA capture strand creates a complex with Ni^{2+} in which two coordination spots bind two histidines in the His_6 tag. Signal detection is achieved by AuNPs conjugated with the complementary DNA strand. **B**: Covalent binding of DNA to CBM3-C. The heterobifunctional linker sSMCC allows binding of amino-modified DNA capture strand to the thiol of the C-terminal cysteine. Detection is achieved as in **A**.

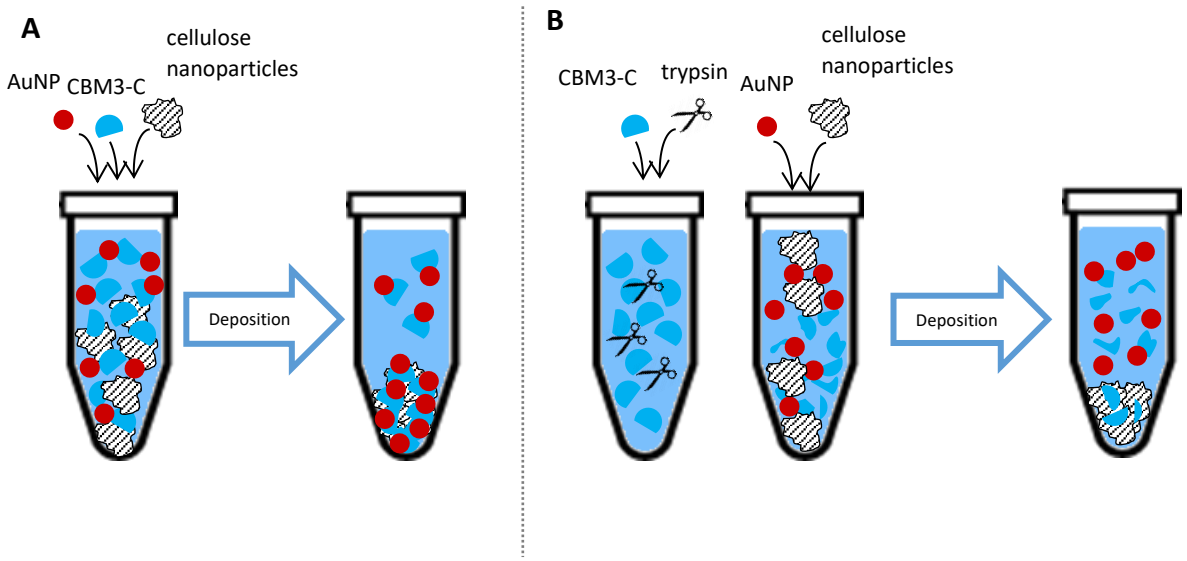

Figure 3: Schematic representation of the proposed CBM-based proteolytic activity sensor. A: Representation of the system without protease addition. The CBM moiety of the CBM3-C construct interacts with cellulose nanoparticles and the available thiol moieties interact with AuNPs. Deposition of cellulose pulls down the CBM bound AuNPs, leading to a decrease of AuNP concentration in the supernatant. **B**: Representation of the system when a protease is added. Pre-incubation of CBM with a protease (e.g., trypsin) leads to CBM proteolysis. Thus, the cellulose-binding and gold-binding moieties will no longer be in the same continuous sequence of amino acid residues. Some cleaved CBMs might still retain cellulose adsorption ability, while some may still bind gold, but after deposition of cellulose, the decrease of AuNP concentration in the supernatant should be lower than in the absence of protease.

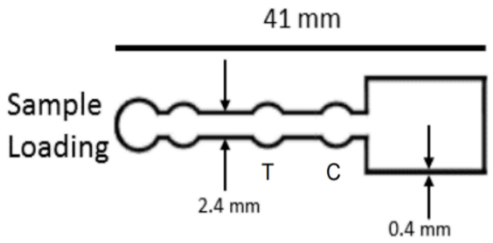

Figure 4: Design of the µPAD for detection of DNA hybridization. The areas labelled with T and C correspond to the Test and Control spots, respectively. The device is 41 mm long, with 2.4 mm wide channels and 0.4 mm thick wax lines. After wax melting and diffusion, the thickness of the wax barriers increases to 1 mm.

design (Figure 4). The printed wax was melted on a heat plate for two minutes, and the µPAD was ready to use after cooling. The cellulose particles used were cellulose microparticles (Sigmacell 20, 20 µm) and cellulose nanoparticles (Innventia Generation 1 microfibrillated cellulose).

2.2. Oligonucleotides

All oligonucleotides were purchased from STABVIDA, and contain sequences present in the genome of the dengue virus, with the exception of SA30, which is derived from *Escherichia coli* (Table 1).

2.3. Gold nanoparticles (AuNP)

AuNPs were synthesized according to the citrate reduction method published by Turkevich et al[13]. Functionalization of AuNPs with oligonucleotides was attained by three different strategies: low pH method, salt aging and freezing. The low pH method involves lowering and then restoring the pH of an AuNP and thiolated DNA mixture. The salt aging method involves a stepwise increase of the NaCl concentration in an AuNP and thiolated DNA mixture up to 300 mM. The freezing method requires a 2h long incubation of the thiolated DNA and AuNP mixture at -20 ºC[14]. AuNP characterization was done by spectrum analysis between 480 nm and 600 nm.

2.4. CBM3-C characterization

The recombinant protein CBM3-C (20.2 kDa) was cloned in *E. coli* by NZYTech, Lda. Growth of *E. coli* accompanied by induction of protein

Table 1: List of oligonucleotides used in this work, with corresponding sequence and modification

Oligo designation	Sequence	5' end modification
SA30	5'-AAAAAAAAAAGTAACGTCAATGAGCAAAGGTATTAACTT-3'	Thiol C6
DSH	5'-TTGAAGTCGAGGCCTGTTCTCGGAGAG-3'	Thiol C6
D3N	5'-CTCTCCGAGAACAGGCCTCGACTTCAA-3'	3x Amino-serinol
DS3	5'-CCTGTTCTCGGAGAG-3'	Thiol C6
DT3	5'-CTCTCCGAGAACAGGCCTCGACTTCAA-3'	None
D3N3	5'-TTGAAGTCGAGG-3'	3x Amino-serinol
DN3	5'-TTGAAGTCGAGG-3'	Amino-serinol

expression was accomplished, and the protein was purified by Immobilized Metal Affinity Chromatography in an ÄKTA 10 Purifier LC system (GE Healthcare). The cellulose-binding ability of CBM3-C was assayed in a suspension of cellulose microparticles, measuring differences in protein concentration before and after particle deposition. The presence of the C-terminal cysteine was confirmed by exploiting the affinity of gold to thiol, adapting the previous assay to measure the spectrum of AuNPs in the supernatant after cellulose particle deposition. Tests were repeated with cellulose nanoparticles, different CBM3 fusions and with DNA-functionalized AuNPs. Results were confirmed with tests on paper support.

2.5. Development of CBM3-C:DNA conjugates

The conjugation of CBM3-C with DNA can be accomplished in two ways: one method relies on establishing a nickel complex between the histidine tag in CBM3-C and tris-nitrilotriacetic acid (NTA)-modified DNA, according to the protocol developed by Goodman et al[15]. Briefly, tris-aminated oligonucleotides (D3N/D3N3) were incubated with 3'3-dithiobis(sulfosuccinimidyl propionate) (DTSSP), for 1 hour, followed by 15-minute incubation with the reducing agent tris(2-carboxyethyl)phosphine (TCEP), in order to originate three thiol moieties. Then, the mixture was incubated with excess NTA-maleimide for 1 hour, thus resulting in three NTA moieties. Synthesis was done in non-aminated, non-thiolated phosphate buffer. The modified oligonucleotide mixture was analyzed by urea-denaturing polyacrylamide gel electrophoresis and stained with ethidium bromide. Conjugation of oligonucleotides with CBM3-C was done by mixing the biomolecules in a 3:2 concentration ratio, respectively, using a small nickel excess in TN buffer (10 mM Tris, 100 mM NaCl, pH 8). Conjugates, protein and oligonucleotide were analyzed by size exclusion chromatography (SEC), with TN buffer running at a 0.5 mL/min.

The second conjugation method relies on establishing a covalent bond between the oligonucleotide and the C-terminal cysteine in CBM3. This is done by introducing a maleimide moiety in aminated DNA (DN3) via incubation with sulfosuccinimidyl 4-[*N*-maleimidomethyl]cyclohexane-1-carboxylate (sSMCC). Conjugation of oligonucleotide and protein was done under the same buffer and concentration ratios as above mentioned.

2.6. Capture systems for DNA recognition

A 2-oligonucleotide system was designed in which a CBM3-C:D3N conjugate was immobilized on the test spot of the fabricated µPAD, which recognized a complementary strand (DSH) immobilized in AuNPs. In the control spot, TST buffer (50 mM Tris, 150 mM NaCl, 0.05% (v/v) Tween 20, pH 7.6) was added. After controls with a non-complementary strand (SA30) bound to AuNPs were performed, conjugate was also deposited in the control spot, at different quantities than in the test spot.

A 3-oligonucleotide was designed in which a CBM3-C:D3N3 or CBM3-C:DN3 conjugate was immobilized on the test and control spots of the fabricated µPAD, which captured a complementary unmodified target DNA strand (DT3), which was then detected by a complementary DNA strand (DS3) immobilized in AuNPs. Controls with a non-complementary strand bound to AuNPs and without target strand were also performed.

All µPADs were digitalized and processed using the imaging processing software Image J (National Institutes of Health). Images were converted to 8-bit grey scale, the colors were inverted and the mean and max grey intensities of the test regions were measured.

2.7. Proteolytic activity sensor

This system is similar to the AuNP binding assay described in section 2.4. The influence of different concentrations of trypsin from bovine pancreas on the spectra of AuNP was analyzed. The spectra of the supernatant of AuNP binding assays via CBM3-C were measured after 5 minutes up to 1-hour pre-incubations of CBM3-C with trypsin.

3. Results and discussion

3.1. Characterization of the CBM3-C fusion protein

The CBM3 from *C. thermocellum* was chosen as the basis for the CBM3-C construct due to its very good binding to cellulose[16]. The CBM3-C fusion protein retained the ability to bind cellulose (results not shown).

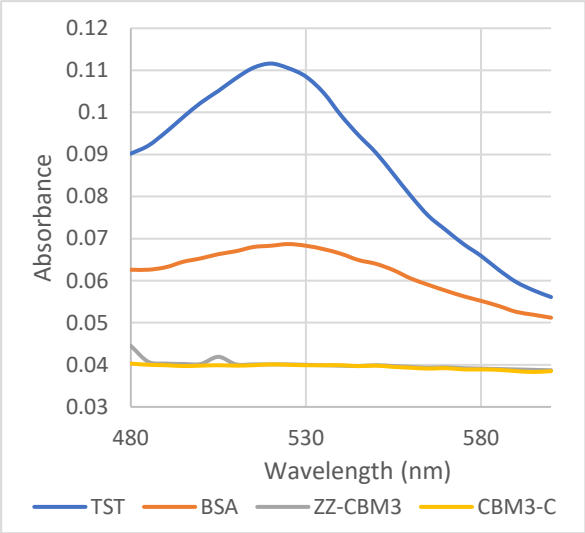

Figure 5: Spectrophotometric analysis of supernatants obtained after settling of cellulose microparticles by gentle centrifugation. Spectra are shown for supernatants obtained after performing pull-down assays with cellulose microparticles and AuNPs and i. TST, ii. BSA, iii. ZZ-CBM3 and iv. CBM3-C. One mg Sigmacell cellulose, 200 µL of 5 µM protein solution and 25 µL of a 10 nM suspension of AuNPs were used in these assays.

The ability of the CBM3-C protein to bind AuNPs via thiol moieties was assayed. In fact, depletion of AuNPs from the supernatant of a cellulose particle suspension was observed after particle deposition (Figure 5). AuNP pull-down assays with the non-thiolated CBM64 from *Spirochaeta thermophila* were also performed. The supernatants resulting from these assays showed identical absorbances to the assays with CBM3-C (Figure 6). This result was unexpected due to the lack of thiols in CBM64. However, interaction between the AuNPs and nitrogen atoms in CBM64 is possible, albeit weaker than gold-sulfur interactions[17].

In order to clarify this issue, similar assays were performed but using AuNPs functionalized with thiolated DNA strands via gold-sulfur interactions. The presence of this DNA coat should hinder the binding of cysteine-containing proteins, and hence the pull-down of AuNPs to cellulose. Nevertheless, since the gold-sulfur interaction is labile, cysteine containing proteins could displace the surface DNA[18], and thus promote the pull-down of some AuNPs to the cellulosic pellet. On the other hand, this displacement should not occur when using proteins with no cysteines like CBM64 – in this case the majority of AuNPs should maintain the integrity of their DNA coat and thus remain in solution. This was confirmed to be the case in Figure 7. AuNP binding ability of CBM3-C was confirmed on tests in paper support. The ability to bind divalent cobalt was also attested and circular dichroism studies posit that its secondary structure remained similar to CBM3.

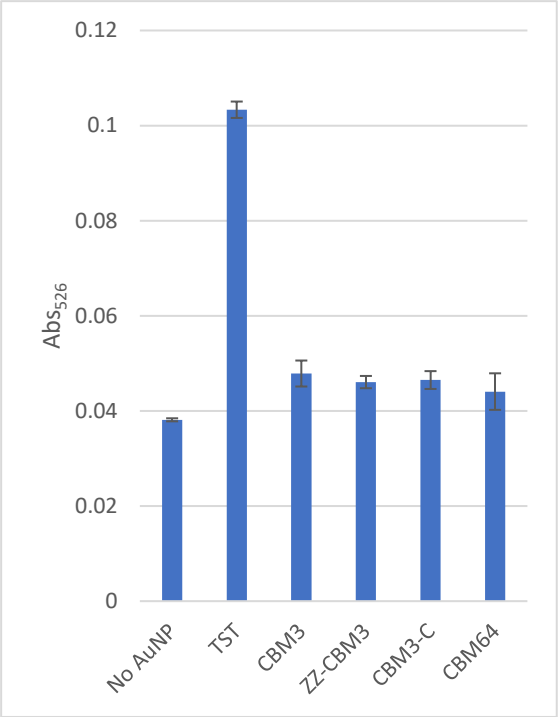

Figure 6: Probing for gold-thiol interactions between AuNPs and different CBM and CBM fusions using pull-down assays with cellulose microparticles. The peak absorption at 526 nm is shown for supernatants obtained after performing pull-down assays with cellulose particles, AuNPs and the indicated proteins. One mg of nanocellulose, 200 µL of 5 µM protein solution and 25 µL of a 10 nM suspension of AuNPs were used in these assays. Data are reported as mean ± standard deviation (n=3).

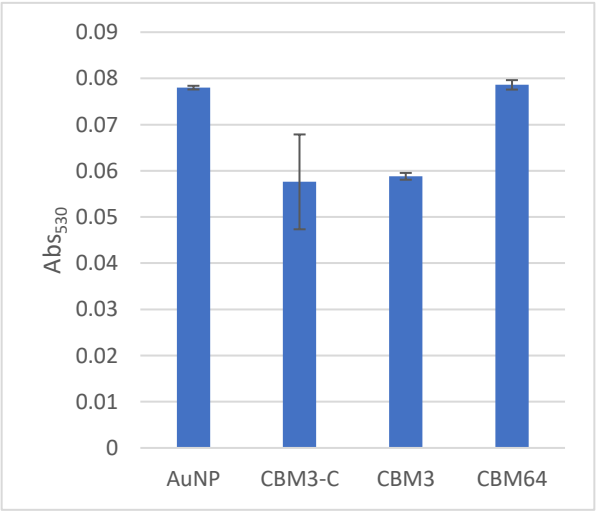

Figure 7: Peak (530 nm) absorbance of supernatants obtained after cellulose/AuNP pull-down assays using salt-aged DNA-functionalized AuNP. The absorbance was measured at 530 nm due to the redshift of the spectrum of functionalized DNA. One mg of nanocellulose, 200 µL of 5 µM protein solution and 25 µL of a 10 nM suspension of AuNPs were used in these assays. Data are reported as mean ± standard deviation (n=3).

3.2. DNA recognition system: non-covalent formation of CBM3-C:DNA conjugate

The conjugation of CBM3-C with DNA oligonucleotides occurs via complexation of nickel by histidines and the tertiary amine of NTA. For every nickel ion, two coordination spots are occupied by the organic nitrogens of the imidazole moieties of two histidines and the remaining four spots are occupied by three carboxylic oxygens and the nitrogen in the tertiary amine of NTA. Thus, modifying DNA with three NTA moieties allows the establishment of three complexes, with all the six histidines in the tag interacting with nickel ions.

Synthesis of NTA-modified oligonucleotides was performed as described in section 2.5. Modification results in an increase of 1491 g/mol in molecular weight when comparing to the original, non-modified oligonucleotide. The reaction mixture was analyzed through urea-denaturing PAGE. (Figure 8). The image of the gel stained with ethidium bromide clearly shows four bands of DNA. The fainter bottom band most likely corresponds to unreacted DNA. The middle two bands are the strongest, indicating that most DNA is in the form of mono- and bisNTA-modified oligonucleotides. Howeves, some of the DNA is in the form of trisNTA-modified oligonucleotides, as indicated by the presence of the topmost band. These result indicates that the synthesis method might require some modifications in order to increase the yield of trisNTA-modified oligonucleotides.

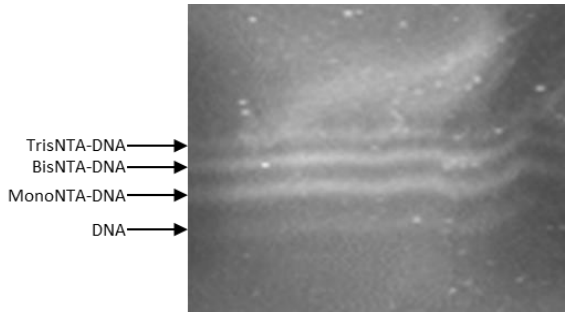

Figure 8: Separation of fully and partially NTA-modified D3N oligonucleotides by urea denaturing gel. The gel was stained with ethidium bromide. Four distinct bands can be seen that likely correspond to tris-, bis-, mono- and non NTA-modified DNA, from top to bottom, respectively.

Conjugation of CBM3-C and DNA was performed under 15% nickel excess following the instructions described in section 2.5. A sample of the conjugate mixture was analyzed by size exclusion chromatography and compared to samples containing only the oligonucleotide and CBM3-C (Figure 9). The chromatogram shows

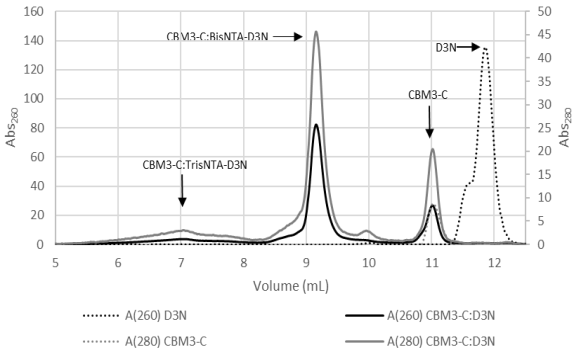

Figure 9: Size exclusion chromatography analysis of the D3N oligonucleotide, CBM3-C and CBM3-C:D3N conjugate. The black and grey dotted lines correspond to the absorption at 260 nm for the D3N oligonucleotide and at 280 nm for CBM3-C, respectively. The black and grey full lines represent the absorption of the CBM3-C:D3N conjugate at 260 nm and 280 nm, respectively.

that the D3N oligonucleotide elutes just before 12 mL, while CBM3-C elutes at 11 mL. Looking at the difference in molecular weights between D3N and CBM3-C (10.5 kDa *versus* 20.2 kDa), a larger difference in elution volume would be expected, since size is the main driving force behind separation in a SEC process. The results of the analysis of the CBM3-C:D3N conjugate mixture show that there is still some unconjugated CBM3-C, as confirmed by the presence of a peak at 280 nm at 11 mL. Additionally, a tall peak is observed at around 9 mL and a small peak is observed at 7 mL. These should correspond to conjugates of CBM3-C with bisNTA-modified D3N and tris-modified D3N, respectively, as indicated by the relative concentrations of the two oligos in Figure 8, backed by some preliminary studies showing that the interaction between monoNTA-modified D3N and CBM3-C is notoriously weak, being unable to form any conjugates (results not shown).

The ability of the CBM3-C:DNA conjugate to capture complementary DNA was tested on the designed µPADs (Figure 4). At first, the objective was to capture the fully complementary DSH DNA strand (Table 1), which was functionalized onto AuNPs. The CBM3-C:DNA conjugate was compared to a similar conjugate prepared with the CBM64 construct. The conjugate was applied to the test spot while TST buffer was applied to the control spot. A control was performed using a non-complementary strand (SA30) immobilized on AuNPs. The images of the µPADs are shown in Figure 10. Capture of the DSH strand was observed in the µPAD modified with the CBM3-C conjugate and tested with the functionalized AuNPs, as signaled by the red color in the test area (Figure, top left). On the contrary, no color

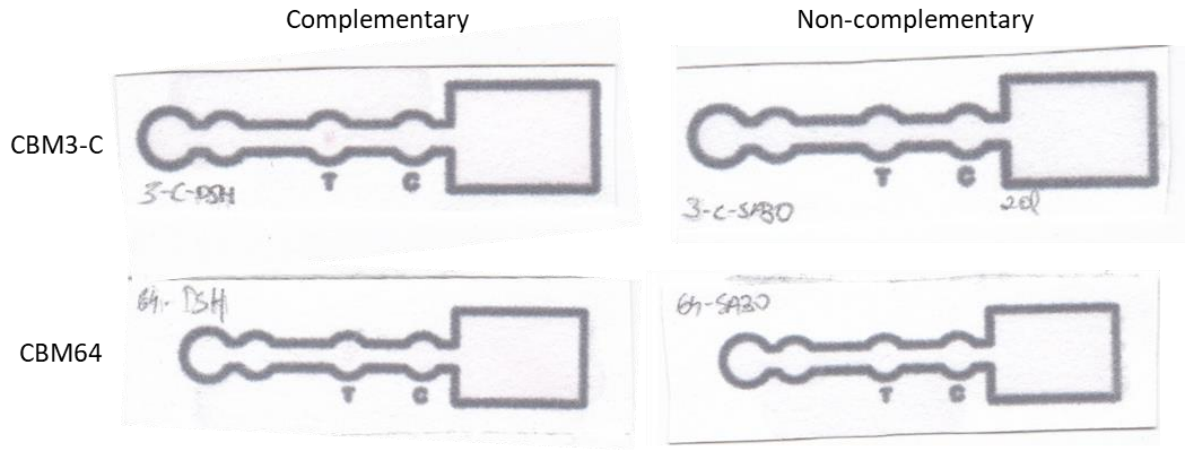

Figure 10: Capture of target DNA strands using µPADs modified with CBM3-C:D3N and CBM64:DNA conjugates. Tests were performed using with AuNPs functionalized with complementary and non-complementary DNA strands**.** Clockwise starting from top left: CBM3-C:D3N tested with AuNPs functionalized with the complementary DNA strand DSH; CBM3-C:D3N tested with AuNPs functionalized with the non-complementary DNA strand SA30; CBM64:D3N tested with AuNPs functionalized with the non-complementary DNA strand SA30; CBM64:D3N tested with AuNPs functionalized with the complementary DNA strand DSH. In all tests pictured above only TST was deposited in the control spot. 5 pmol of each conjugate were deposited in the test spot.

was observed in the µPAD that was tested with AuNPs functionalized with the non-complementary SA30 strand. Thus, it is possible to conclude that this system of nickel-mediated complex between NTA-modified oligonucleotides and CBM3-C can accurately capture complementary DNA strands on a paper support. The µPAD modified with the CBM64 conjugate also produced a signal when tested with the DSH-functionalized AuNPs, but this was fainter and thus is barely perceptible in the figure above (bottom left).

The conjugation process was then optimized by analyzing the positive signal produced by conjugates formed with different excesses of nickel (15% to 100%). Conjugation performed at 25% nickel excess was chosen as preferable, since it showed the clearer signal to the naked eye (results not shown).

3.3. DNA recognition system: covalent formation of CBM3-C:DNA conjugate

Conjugation of DNA with CBM3-C was also accomplished by establishing a bond between the C-terminal thiol moiety in the cysteine residue of CBM3-C and a maleimide-modified oligonucleotide. The modified oligonucleotide was obtained by adding sSMCC to a mono-aminated oligonucleotide (DN3), as described in section 2.5. Modification resulted in an increase of 219 g/mol in the molecular weight of the starting nucleotide. After modification, oligonucleotides were combined with CBM3-C at a 3:2 ratio, as used earlier in the nickel-mediated formation of conjugates.

A different capture system was tested using this conjugate, a 3-oligonucleotide capture system. In this system, a smaller oligonucleotide (DN3, Table 1) is immobilized in a CBM3-C conjugate. This oligonucleotide is quite smaller (12 nucleotides) than the D3N oligonucleotide (27 nucleotides) used in the 2-oligonucleotide strategy. The construct is then used to recognize a longer, unmodified complementary DNA strand, the DT3 oligonucleotide (Table 1), forming a double strand with roughly half of the DT3 strand. The other half

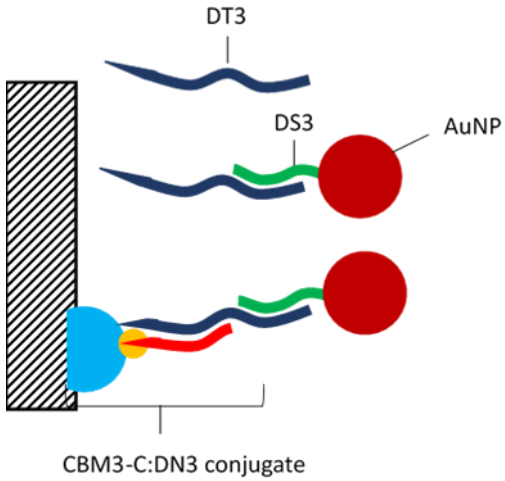

Figure 11: Schematic representation of the 3-oligonucleotide DNA recognition system. An unmodified DNA strand, DT3, is added to the µPAD, which hybridizes with the smaller, complementary DS3 strand, functionalized onto AuNPs. The DN3 strand conjugated via covalent coupling with CBM3-C recognizes the DT3 target strand by hybridization with the remaining sequence of DT3 that did not hybridize with DS3. So, DN3 will be the capture strand, DT3 the target strand and DS3 the detection strand. A scheme for a 3-oligonucleotide DNA recognition system based on a CBM3-C conjugated prepared via nickel complexation would be similar, only switching the DN3 oligonucleotide for the D3N3 oligonucleotide.

of the DT3 strand is then hybridized with a smaller DNA oligonucleotide that was functionalized onto AuNPs (DS3, Table 1). A schematic representation is shown in Figure 11. The system was tested in parallel using nickel-based conjugates prepared with the D3N3 oligonucleotide, which presents the same sequence of nucleotides as DN3, but is tris-aminated. These conjugates were tested on µPADs similarly to section 3.2., and controls were performed by running µPADs i) with AuNPs functionalized with the non-complementary oligonucleotide SA30 and ii) without addition of the DT3 target.

Results showed that the nickel-based complex was capable to accurately detect AuNPs capped with the complementary DS3 strand, while giving no signal when AuNPs were functionalized with the non-complementary SA30 strand. The tests with the covalently-formed complex, on the other hand, resulted in positive signals with AuNPs functionalized with both complementary and non-complementary oligonucleotides, thus indicating that AuNP binding is not discriminatory in covalently-linked conjugates. The control performed without the target strand, DT3, also presented a positive signal, which was unexpected due to the absence of an integral oligonucleotide. However, this can be explained due to some complementarity between the detection (DS3) and capture strands (D3N3/DN3). As 50% of the DN3N/DN3 oligonucleotide is complementary to the DS3 oligonucleotide, direct interaction between the capture and the detection strand is possible. As there is no target strand, this system became a 2-oligonucleotide system, in which non-fully complementary DNA strands are also captured and detected.

In an effort to prevent this partial hybridization, the µPAD tests were repeated with an added step of washing with a low salt buffer after conjugate deposition. The washing steps reduced the signal when the system is complete, but did not present significant differences without the target strand, in the case of the covalently linked conjugate. On the other hand, the washings removed all capability of detection from the nickel-mediated complex, not producing a signal with or without the target strand.

3.4. Proteolytic activity sensor

The other proposed biosensor is a proteolytic activity sensor, using the non-specific protease trypsin as proof-of-concept (Figure 3). In order to do so, the influence of trypsin concentration of the spectrum of AuNPs was first assessed. The spectra of supernatants of a mixture of cellulose nanoparticles, AuNPs, and trypsin at different concentrations were measured after deposition of the cellulose nanoparticles by gentle centrifugation (Figure 12).

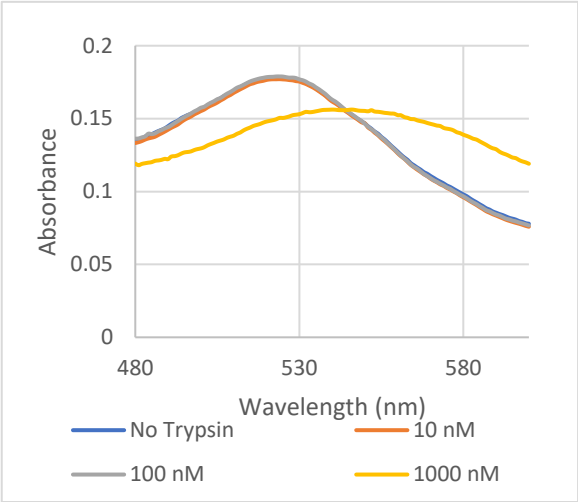

Figure 12: Effect of trypsin concentration on the spectra of AuNP-containing supernatants. Spectra shown are the mean of three separate measurements.

No variations in the spectra obtained with 10 and 100 nM of trypsin were detected when compared with a control spectra obtained with no trypsin. However, 1000 nM of trypsin produced a redshift of the absorption band from around 525 nm to around 546 nm. Thus, the sensor design is not suitable for sensing proteolytic activity of trypsin at concentrations as high as 1000 nM, as the trypsin itself interferes with the AuNP spectrum.

Further tests were conducted with a final trypsin concentration of 10 nM, as it was thought to give better sensitivity to the sensor. CBM3-C was incubated with trypsin for different time intervals, and then cellulose nanoparticles and AuNP were added to the solution. Figure 13 shows the spectra of the supernatants recovered after gentle centrifugation corresponding to incubations of 5, 15, 30 and 60 minutes. One thing of note to take from Figure 13 is that in the spectrum of the assays without trypsin a redshift to 540 nm is also observed. Further tests showed that this redshift is caused by the addition of CBM3-C. Thus, non-adsorbed CBM3-C interacts with AuNPs via thiol-gold interactions, giving rise

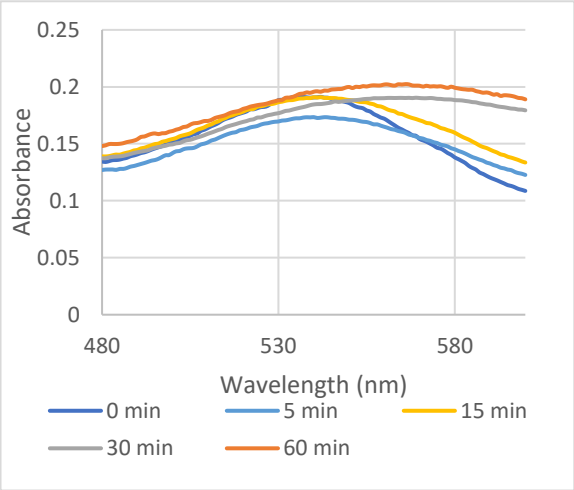

Figure 13: Effect of time of CBM3-C incubation with trypsin on the spectrum of supernatants. Spectra shown are the mean of three separate measurements. Control with 0 min incubation was done without trypsin. Spectra from assays with 2, 3 and 4-hour-long incubations are similar to the spectra of 30 and 60-minute-long incubation, and thus are not shown for increased readability.

to this redshift. The assays with 5 and 15-minute-long incubations have similarly shaped spectra to the control, with their absorbance peaks around 540 nm. However, a difference in intensity is observed. The assay with 15-minute-long incubation has an absorbance value similar to the no incubation control, so no particles should be adsorbed via CBM3-C to the cellulose phase. On the other hand, an incubation for 5 minutes displays lower absorbance, meaning that some AuNPs are in the cellulose phase. As the incubation time was lower, fewer CBM3-C were cleaved by trypsin, allowing some deposition of AuNPs together with the cellulose nanoparticles. Spectra from assays with 30-minute or longer incubations show a considerable redshift due to aggregation of AuNPs, which was also observed to the naked eye thanks to a change of color of the supernatant from red to purple. The increased incubation time leads to a more extensive digestion of CBM3-C and autolysis of trypsin, creating smaller peptides. The more diminutive size of these peptides should allow a bigger number of interactions with AuNPs, since they do not occupy as much space around AuNPs as the native proteins, eventually causing aggregation. The choice for performing these tests with 10 nM trypsin proved to be sensible, since an increased concentration of trypsin would most likely require shorter incubations to observe similar results.

6. Conclusions

The objectives of this work were to develop paper-based biosensors using CBM3-C, a fusion protein that combines a family 3 CBM from *Clostridium thermocellum* with a N-terminal His_6 tag and a C-terminal cysteine. This fusion was characterized in regard to its cellulose binding, establishment of gold-thiol interactions with AuNPs, formation of metallic complexes via His_6 tag and overall secondary structure. CBM3-C maintained the capability of CBM3 to bind to cellulose and successfully bound both citrate-capped and DNA functionalized AuNPs.

CBM3-C was then incorporated into a paper-based biosensor designed for cDNA recognition. First, conjugates of CBM3-C with DNA capture strands were assembled by either exploring the presence of the His_6 tag or of the terminal cysteine, by non-covalent and covalent approaches, respectively. Detection systems were then conceived to test the ability of the DNA strand in the CBM3-C:DNA conjugates to capture complementary target DNA strands in wax-printed µPADs. In a first instance, the nickel complex conjugate was immobilized in the µPAD and used to capture AuNPs functionalized with thiolated DNA strands. Positive signals were obtained when AuNPs were functionalized with complementary DNA strands, while no signal was observed with non-complementary strands.

A 3-oligonucleotide system was also designed that required no modification of the target DNA. Here, detection was performed using AuNPs functionalized with a smaller complementary DNA strand. µPAD tests using this system resulted in more dubious results. Although the nickel complex conjugate accurately detected the target strand when AuNPs were functionalized with complementary strands, producing no signal when AuNPs were functionalized with non-complementary strands, the tests resulted in a positive signal when the target strand was not included. Similar results were observed when using the covalent conjugate, although this seemed to be less discriminatory than the former conjugate, yielding a positive signal even when AuNPs are functionalized with non-complementary DNA. Washing of the sensors resulted in a complete loss of capture ability by the nickel complex conjugate, while no considerable difference was observed for the covalent conjugate. In the future, this system should be tested using different oligonucleotides that are less complementary, as the complementary strand bound to AuNPs did possess some complementarity to the capture strand conjugated to CBM3-C. Furthermore, the 3-oligonucleotide system would be more similar to what could eventually be used in POC applications, as it uses an unmodified DNA target.

A second biosensor was used to measure proteolytic activity. As CBM3-C simultaneously bound to cellulose (via CBM) and AuNPs (via thiol moiety), the introduction of a non-specific protease should break this cellulose-CBM-AuNP chain. This was measured in a suspension of cellulose nanoparticles, to which AuNPs and CBM3-C that was previously incubated with trypsin were added. Analysis of the spectra of the supernatant measured after deposition of cellulose should give a clue to the extent of proteolytic activity, as a more extensive reaction results in a larger concentration of AuNPs in the supernatant, leading to AuNP aggregation in the long run. This device was meant to be a proof-of-concept and, as such, it was successful. In the future, a similar assay can be performed for drug design against a specific protease, as a target amino acid sequence can be introduced as a linker between CBM and a signal molecule, providing a simple assay for testing drug inhibition of proteases.

Acknowledgments

This work was performed at the Institute for Bioengineering and Biosciences of Instituto Superior Técnico (Lisbon, Portugal), during the period October 2018-July 2019, under the supervision of Prof. Miguel Prazeres and in the context of the project “CBM-X: Biorecognition as a Tool for the Functionalization of Cellulose-based Materials with Biomolecules and Nanostructures” (PTDC/CTM-CTM/30790/2017), funded by Fundação para a Ciência e Tecnologia.

References

1.Commission on a Global Health Risk Framework for the Future & National Academy of Medicine, S. The Neglected Dimension of Global Security. (National Academies Press (US), 2016). doi:10.17226/21891

2.Kosack, C. S., Page, A.-L. & Klatser, P. R. A guide to aid the selection of diagnostic tests. Bull World Heal. Organ 95, 639–645 (2017).

3.Cate, D. M., Adkins, J. A., Mettakoonpitak, J. & Henry, C. S. Recent Developments in Paper-Based Microfluidic Devices. Anal. Chem. 87, 19–41 (2015).

4.Boraston, A. B., Bolam, D. N., Gilbert, H. J. & Davies, G. J. Carbohydrate-binding modules: fine-tuning polysaccharide recognition. Biochem. J. 382, 769–781 (2004).

5.Shoseyov, O., Shani, Z. & Levy, I. Carbohydrate Binding Modules: Biochemical Properties and Novel Applications. Microbiol. Mol. Biol. Rev. 70, 283–295 (2006).

6.Armenta, S., Moreno-Mendieta, S., Sánchez-Cuapio, Z., Sánchez, S. & Rodríguez-Sanoja, R. Advances in molecular engineering of carbohydrate-binding modules. Proteins Struct. Funct. Bioinforma. 85, 1602–1617 (2017).

7.Ficko-Blean, E. & Boraston, A. B. Insights into the recognition of the human glycome by microbial carbohydrate-binding modules. Curr. Opin. Struct. Biol. 22, 570–577 (2012).

8.Tolba, M. et al. Oriented Immobilization of Bacteriophages for Biosensor Applications. Appl. Environ. Microbiol. 76, 528–535 (2010).

9.Hinkley, T. C. et al. Reporter bacteriophage T7NLC utilizes a novel NanoLuc::CBM fusion for the ultrasensitive detection of: Escherichia coli in water. Analyst 143, 4074–4082 (2018).

10.Rosa, A. M. M. et al. Capture and Detection of DNA Hybrids on Paper via the Anchoring of Antibodies with Fusions of Carbohydrate Binding Modules and ZZ-Domains. Anal. Chem. 86, 4340–4347 (2014).

11.Rosa, A. M., Nazaré, M. R. & Prazeres, D. M. Colorimetric detection of DNA strands on cellulose microparticles using ZZ-CBM fusions and gold nanoparticles. Biotechnol. J. 1800590, 1800590 (2019).

12.Zhou, W., Gao, X., Liu, D. & Chen, X. Gold Nanoparticles for In Vitro Diagnostics. Chem. Rev. 115, 10575–10636 (2015).

13.Turkevich, J., Stevenson, P. C. & Hillier, J. A study of the nucleation and growth process in the synthesis of colloidal gold. Discuss. Faraday Soc. 55, 55–75 (1951).

14.Liu, B. & Liu, J. Freezing Driven DNA Adsorption on Gold Nanoparticles: Tolerating Extremely Low Salt Concentration but Requiring High DNA Concentration. Langmuir acs.langmuir.9b00746 (2019). doi:10.1021/acs.langmuir.9b00746

15.Goodman, R. P. et al. A Facile Method for Reversibly Linking a Recombinant Protein to DNA. ChemBioChem 10, 1551–1557 (2009).

16.Pires, V. M. R. R. et al. Stability and Ligand Promiscuity of Type A Carbohydrate- binding Modules Are Illustrated by the Structure of Spirochaeta thermophila St CBM64C. J. Biol. Chem. 292, 4847–4860 (2017).

17.Mollenhauer, D. Nitrogen- and phosphine-binding ligands in interaction with gold atoms, clusters, nanoparticles and surfaces. in Chemical Modelling 12, 293–350 (2016).

18.Bürgi, T. Properties of the gold-sulphur interface: from self-assembled monolayers to clusters. Nanoscale 7, 15553–15567 (2015).